

Fast Memory-Efficient Full-Wave 3D Simulation of Power Planes

Narayanan T.V., Krishna Srinivasan, Madhavan Swaminathan

*School of Electrical and Computer Engineering
Georgia Institute of Technology, Atlanta, GA, USA*

{ntv, krishna, madhavan.swaminathan}@ece.gatech.edu

Abstract— A circuit-equivalent frequency-domain electromagnetic simulation for packaging structures is proposed. Simulations are carried out using an iterative memory-efficient approach – quasi-minimal residual method. The convergence of the solver is accelerated by the use of a suitable preconditioner. Results for a power-plane example, with and without aperture, are presented.

I. INTRODUCTION

The analysis of power-ground structures presents a significant problem in signal/power integrity as well as for electromagnetic interference (EMI) considerations [1] [2]. Such problems have been analyzed in the past by making use of time- and frequency- domain techniques. Most of these solvers can be classified, in increasing order of accuracy, as two-dimensional (2D) [3], two-point-five –dimensional (2.5D) [4] and three-dimensional (3D) [5]. Though 3D solvers are the most accurate, they also impose a heavy penalty in terms of time required for analysis. At a lower level, lumped circuit models for such structures have also been proposed [6]. The parameterization of these lumped-circuit models can then help in the fast analysis of very large structures. Thus a hierarchical approach to the design and analysis of such problems is best – at the first stage, lumped circuit models can be used followed by analysis with 2D or 2.5D solvers. This is then followed up with full-wave solution as the final verification step for fine-tuning before the actual fabrication.

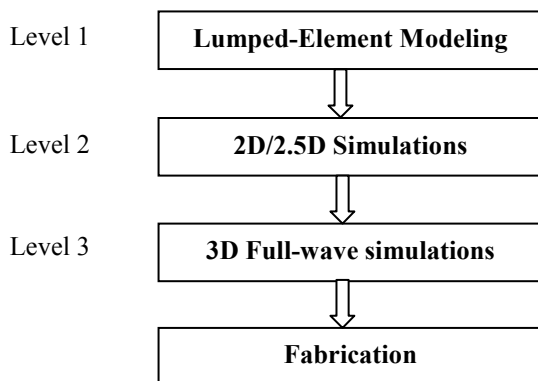


Fig.1 Hierarchical design flow based on simulation complexity affording more design iterations at lower levels

Some of the full-wave approaches that have been investigated include – finite difference, finite element, and spectral domain, to name a few. Finite-difference time-domain (FDTD) in particular, has been extensively studied and used for various applications [7], because of its flexibility and ability to simulate high frequency behavior. On the other hand, work on finite-difference based frequency domain simulation tools is limited. Frequency domain simulation offers several advantages: 1) Accurate simulation of low frequency characteristics 2) Easier incorporation of frequency-dependent material parameters and 3) Elimination of post-processing steps to extract equivalent circuits, as opposed to FDTD where transformation to frequency-domain with appropriate use of windowing is required.

The solution to the frequency domain Maxwell's equation presents what is called an inverse problem. Such problems are usually time-consuming. However, due to the sparse nature of the matrix, fast direct solvers can be exploited [8]. But, as the problem sizes begin to grow, the analysis becomes increasingly difficult due to prohibitive memory requirements. Iterative solutions are therefore used in such cases [9]. Two of the most popular algorithms used are the conjugate gradient method and the bi-conjugate gradient method [10]. However, for the current problem, both these techniques face convergence issues. Therefore the quasi-minimal residual (QMR) method [11] is used. In conjunction with preconditioning techniques, it provides for a quicker convergence, thus making possible a memory-efficient fast simulation of power/ground structures.

This paper proposes an electromagnetic simulation method by converting the Maxwell's equations into an electrical equivalent network for the analysis of metal plane structures. This offers the advantages of 1) making use of Spice-based circuit solvers to run full-wave simulations and 2) using circuit based numerical techniques to speed-up the simulation. Further, the use of QMR approach for solving such problems is analyzed and performance improvement is demonstrated by making use of a diagonal preconditioner. The paper is organized as follows: Section II describes the formulation of the equivalent circuit based simulator along with the QMR algorithm. Section III details the results and discussion.

II. FORMULATION

A. Maxwell's Equations Discretization

Consider the differential form of Maxwell's equation in the frequency domain

$$\nabla \times \mathbf{E} = -j\omega\mathbf{B} \quad (1)$$

$$\nabla \times \mathbf{H} = j\omega\mathbf{D} \quad (2)$$

where, \mathbf{E} and \mathbf{H} are the vector electric and magnetic fields

\mathbf{D} and \mathbf{B} are the vector electric and magnetic field densities

ω is the frequency in radians

Assuming an isotropic, lossless and homogeneous medium, the above equations can be written for a two-dimensional (2D) transverse magnetic (TM) wave as:

$$j\omega\varepsilon E_z = \frac{\partial H_y}{\partial x} - \frac{\partial H_x}{\partial y} - J_z \quad (3)$$

$$j\omega\mu H_x = -\frac{\partial E_z}{\partial y} \quad (4)$$

$$j\omega\mu H_y = \frac{\partial E_z}{\partial x} \quad (5)$$

where, ε and μ are the material permittivity and permeability, respectively

E_p and H_p represent the electrical and magnetic field in the p-direction ($p = x$ or y or z).

J_z is the external current source in the z-direction

Discretizing the above equations using the Yee-grid, so as to implicitly satisfy the divergence laws, we can form an electrical equivalent circuit for the resulting equations as shown in Fig. 2. The nodal voltages represent the electrical fields and the magnetic fields map to the branch currents. The circuit branch connected to ground can be further simplified to an equivalent Norton circuit, thus reducing the problem to one of solving only for the nodal voltages. The solution of the electrical network results in a linear equation of form $\mathbf{Ax} = \mathbf{b}$ where \mathbf{A} is the sparse and banded nodal analysis (NA) amplification matrix, \mathbf{x} is the vector of unknown nodal voltages and \mathbf{b} is the vector containing external current sources.

The analysis of the circuit network can be done at discrete frequencies using NA. The resulting admittance matrix gives rise to an $O(N^2)$ direct problem, where N is the number of nodes. The complexity can be further reduced by making use of suitable sparse solvers. In addition, the circuit representation allows the use SPICE-based circuit solvers for frequency-domain full-wave simulation. The current-controlled current sources (CCCS) are converted into voltage-controlled current sources (VCCS). This reduces the dimension of the NA matrix, by ensuring that only the nodal

voltages are being solved for, without the addition of the branch currents to the vector \mathbf{x} .

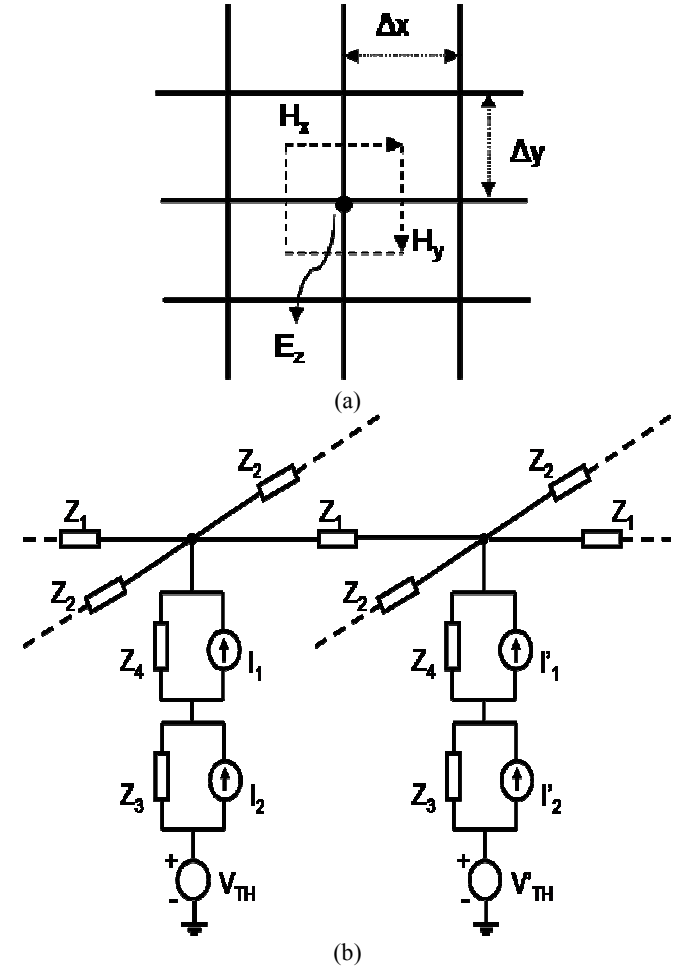


Fig.2 (a) Yee-grid unit-cell and (b) its equivalent-circuit representation for full-wave simulation

The circuit elements in the equivalent network in Fig.2 are given as follows.

Impedances:

$$\begin{aligned} Z_1 &= j\omega\mu\Delta x \\ Z_2 &= j\omega\mu\Delta y \\ Z_3 &= \frac{1}{(j\omega\varepsilon)\Delta x} \\ Z_4 &= \frac{1}{(j\omega\varepsilon)\Delta y} \end{aligned} \quad (6)$$

Dependent Voltage Sources:

$$\begin{aligned} V_{TH} &= \frac{J_{z,ext}(i, j)}{j\omega\varepsilon} \\ V'_{TH} &= \frac{J_{z,ext}(i+1, j)}{j\omega\varepsilon} \end{aligned} \quad (7)$$

CCCS:

$$\begin{aligned}
I_1 &= j\omega\mu\Delta y \begin{pmatrix} V_{i+\frac{1}{2},j+1} & -V_{i+\frac{1}{2},j} \\ & \end{pmatrix} \\
I_2 &= j\omega\mu\Delta x \begin{pmatrix} V_{i,j+\frac{1}{2}} & -V_{i+1,j+\frac{1}{2}} \\ & \end{pmatrix} \\
I'_1 &= j\omega\mu\Delta y \begin{pmatrix} V_{i+\frac{3}{2},j+1} & -V_{i+\frac{3}{2},j} \\ & \end{pmatrix} \\
I'_2 &= j\omega\mu\Delta x \begin{pmatrix} V_{i+1,j+\frac{1}{2}} & -V_{i+2,j+\frac{1}{2}} \\ & \end{pmatrix}
\end{aligned} \tag{8}$$

where, Δx and Δy are the grid spacing along the X- and Y- directions, respectively.

Perfect electric conductor (PEC) and perfect magnetic conductor (PMC) boundary conditions are enforced by shorting and opening the nodal points along the boundaries of the simulation domain, respectively. The above procedure is easily extended to three dimensions and the full-wave 3D solution is used for further analysis in the paper.

B. Quasi Minimal Residual (QMR) Method

The QMR method proposed in [11] is essentially a nonsymmetric Lanczos process based on projection on to a biorthogonal basis in the Krylov subspace. It improves on the convergence behavior of the bi-conjugate gradient (BiCG) and uses look-ahead techniques in the Lanczos process to avoid breakdown. The Lanczos biorthogonalization process [13] is used to generate these subspaces.

The algorithm for generating these subspaces is given in Fig.3.

1. Choose two vectors v_1, w_1 s.t. $(v_1, w_1) = 1$
2. Set $\beta_1 = \delta_1 = 0, w_0 = v_0 = 0$
3. For $j=1,2,\dots,m$, Do
4. $\alpha_j = (Av_j, w_j)$
5. $v_{j+1} = Av_j - \alpha_j v_j - \beta_j v_{j-1}$
6. $w_{j+1} = A^T w_j - \alpha_j w_j - \delta_j w_{j-1}$
7. $\delta_{j+1} = |(v_{j+1}, w_{j+1})|^{1/2}$. If, $\delta_{j+1} = 0$, stop.
8. $\beta_{j+1} = (v_{j+1}, w_{j+1}) / \delta_{j+1}$
9. $v_{j+1} = v_{j+1} / \delta_{j+1}$
10. $w_{j+1} = w_{j+1} / \beta_{j+1}$
11. End Do

Fig.3 The Lanczos biorthogonalization algorithm which forms the basis for the QMR algorithm

This process is then used within the two-sided Lanczos algorithm to solve the linear system,

$$Ax = b \tag{9}$$

where, A is the complex coefficient matrix. If x_0 is an initial guess for x , then r_0 is defined as $r_0 = b - Ax_0$, then the starting vector is chosen as

$$v_1 = \frac{r_0}{\|r_0\|_2} \tag{10}$$

Then the n th Krylov complex subspace generated by v_1 and A are given by

$$K_n(v_1, A) = \text{span}\{v_1, Av_1, \dots, A^{n-1}v_1\} \tag{11}$$

and a corresponding subspace is generated for the transpose of A matrix using a starting vector w_1 such that

$$(v_1, w_1) = 1 \tag{12}$$

The two-sided Lanczos algorithm [13] is described in Fig.4.

1. Compute $r_0 = b - Ax_0$ and $\beta = \|r_0\|_2$
2. Generate the biorthogonal Lanczos vectors (Fig. 1) (i.e., generate vectors $v_1, v_2, \dots, v_m, w_1, w_2, \dots, w_m$ and the tridiagonal matrix T_m)
3. Compute $y_m = T_m^{-1} r_0$ and $x_m = x_0 + V_m y_m$

Fig.4 The two-sided Lanczos algorithm for the solution of linear systems

where, T_m is now defined as the tridiagonal matrix

$$T_m = \begin{bmatrix} \alpha_1 & \beta_2 & & & \\ \delta_2 & \alpha_2 & \beta_3 & & \\ & \cdot & \cdot & \cdot & \\ & & \delta_{m-1} & \alpha_{m-1} & \beta_m \\ & & & \delta_m & \alpha_m \end{bmatrix} \tag{13}$$

The result of the Lanczos process is a relation of the form

$$AV_m = V_{m+1} \bar{T}_m = V_m T_m + \delta_{m+1} v_{m+1} e_m^T \tag{14}$$

Subsequently, a general minimal residual method (GMRES) [12] -like process is used on the result obtained from the Lanczos algorithm. However, unlike the GMRES case, here the basis vectors used are not orthogonal, thus giving rise to the name quasi-minimal residual algorithm. Defining $\Omega_m = \text{diag}(\omega_1, \omega_2, \dots, \omega_{m+1})$, ($\omega_j > 0, j=1,2,\dots,m+1$)

as a diagonal weight matrix, the corresponding residual in the Lanczos process can now be evaluated as

$$r_m = V_{m+1} \Omega_m^{-1} (d_m - \Omega_m \bar{T}_m y_m) \tag{15}$$

where, $d_m = \omega_1 \beta e_1^{m+1}$

The problem is then reduced to the least squares problem

$$\|(d_m - \Omega_m \bar{T}_m y_m)\| = \min \|(d_m - \Omega_m \bar{T}_m y_m)\|, y_m \in \mathbf{C} \tag{16}$$

where, \mathbf{C} is the complex vector space.
The QMR algorithm is outlined in Fig.5.

1. Compute $r_0 = b - Ax_0$ and $\gamma_1 = \|r_0\|_2$, $w_1 = v_1 = r_0 / \gamma_1$
2. For $m=1,2,\dots$, until convergence, Do
3. Perform m iterations of look-ahead Lanczos procedure. This yields matrices V_m, V_{m+1} and \bar{T}_m
4. Update QR factorization of $\Omega_m \bar{T}_m$ and the vector t_m

$$\Omega_m \bar{T}_m = Q_m^H \begin{bmatrix} R_m \\ 0 \end{bmatrix} \quad \text{and} \quad t_m = R_m y_m$$
5. Compute $x_m = x_0 + V_m R_m^{-1} t_m$
6. End Do

Fig.5 The QMR algorithm – implemented by combining the look-ahead Lanczos procedure with a least squares algorithm.

Here the matrix Q_m^H represents the complex conjugate of the matrix Q_m .

The breakdown of iterative algorithms presents an important problem. An exact breakdown of the Lanczos algorithm may occur if

$$(v_1, w_1) = 0. \quad (18)$$

A near-breakdown occurs when the Lanczos vectors are scaled by very small values. The basic concept of the look-ahead algorithm is that, even though the pair (v_{j+1}, w_{j+1}) cannot be defined in a biorthogonal sense, the subsequent pair (v_{j+2}, w_{j+2}) can be successfully defined. This avoids cases of near-breakdown, at the cost of increased computational steps, thus providing for superior convergence of QMR. The other significant advantage of QMR is that the required memory volume does not increase with iteration count, as is the case with minimal residual methods like GMRES. Only two sets of vectors have to be stored during an iteration, as opposed to storing the entire history of the basis vectors.

The convergence of the QMR process can be improved by making use of a preconditioning matrix M . The preconditioning matrix is used as a multiplier, and instead of solving (9), the following equation is solved

$$\mathbf{M}^{-1} \mathbf{A} \mathbf{x} = \mathbf{M}^{-1} \mathbf{b}. \quad (19)$$

A very commonly used preconditioner is the incomplete LU factorization (ILU) of the \mathbf{A} matrix [13]. However, the ILU factorization of the \mathbf{A} matrix in the present case fails to provide a solution [14]. To overcome this issue, the diagonal of the \mathbf{A} matrix is used as the preconditioner.

III. RESULTS AND DISCUSSION

To verify the accuracy of the QMR process, a 13mm x 13mm thin metal plane is considered, placed at the center of a dielectric box of dimensions 21mm x 21mm x 60 μ m. A unit cell of 1mm x 1mm x 10 μ m was used to discretize the structure shown in Fig. 6.

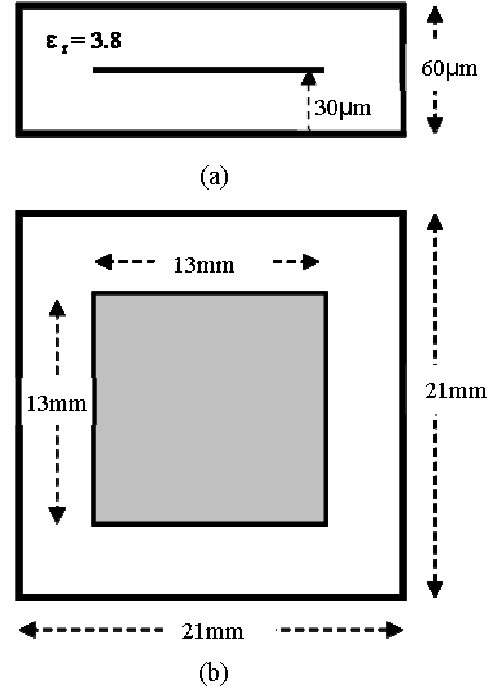


Fig.6 (a) Cross-section and (b) top-view of metal plane structure

A probe is placed at a point 5 μ m below the metal plane and at a distance of 7mm from the PEC boundaries, and is referenced to the bottom PEC. A frequency sweep of the structure is carried from 0.5GHz to 6GHz and the results of the QMR-based solver are compared with those of the direct method. The target residual is set to be 10^{-6} with the maximum number of iterations set at 400.

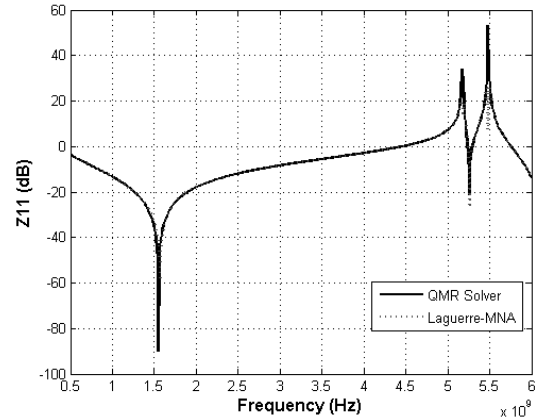


Fig.7 Impedance response of the metal plane structure showing close match between the QMR based approach (solid) and Laguerre-MNA [5] (dashed)

Fig.7 shows a favorable comparison of the QMR solver with a close overlap with the Laguerre solver (Laguerre-MNA) [5] over the entire frequency range, thus validating the solver. The power plane problem gives rise to a square matrix of dimension, $N = 9,372$. Since QMR solver exhibits conjugate gradient-like memory usage properties, i.e., of $O(N \log(N))$, as

opposed to $O(N^2)$ of direct solvers, a comparison is made of the memory used by the solvers themselves for the current problem. The memory used by the direct solver is 49 megabytes (MB) compared to using the QMR solver with preconditioner, wherein only 3.3 MB of memory is required.

Next, a two-metal plane structure with aperture on the top plane is considered. The structure, with PEC boundaries, is shown in Fig.8. The discretization of the 22mm x 22mm x 80 μ m volume is done using a unit cell of 1mm x 1mm x 10 μ m. A probe is placed 5 μ m directly below the edge center of the plane with aperture, referenced to the bottom plane.

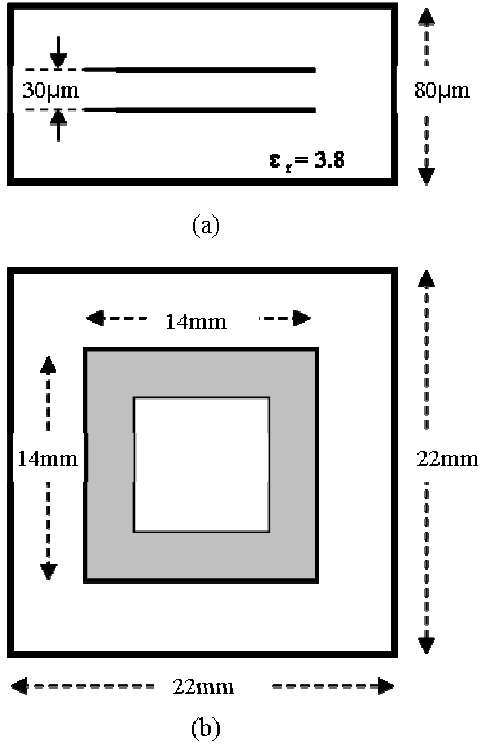


Fig.8 (a) Cross-section and (b) top-view of metal plane structure with aperture. Aperture is present only in the top plane.

Frequency sweep simulations are carried out from 0.5 to 6 GHz, and the results of the QMR-based solver for different residuals are plotted in Fig.9. Frequency steps of 0.1 GHz are used to analyze this structure. From the plot, it is clear that accuracy is reached when the tolerance level is set to 10^{-3} , since the curves of residual equal to 10^{-3} and 10^{-4} overlap. Fig.10 and Fig.11 show the top-view cuts of electric fields 10 μ m above the top metal surface. The fringing fields clearly shown in these plots are accounted for in lower-dimensional solvers by means of analytical expressions and therefore are heavily structure dependent. Thus, in case of analyzing novel layouts, as also in validating lower dimensional simulations, there is a need for 3D simulation.

To analyze the performance improvement with the use of preconditioner, we run the above simulation at 1GHz, with

target residual of 10^{-3} , with and without the use of preconditioner

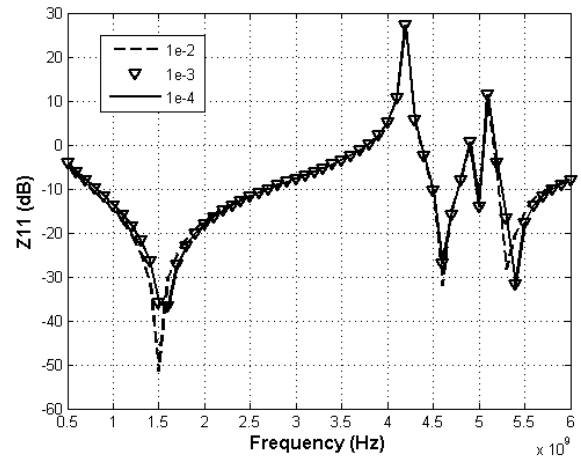


Fig.9 Impedance response plot for the structure shown in Fig.8 for various tolerance levels in the QMR algorithm.

The simulation converges in 462 iterations without the preconditioner, and converges in 216 iterations when the diagonal preconditioner is used. Clearly, the use of preconditioner enables superior convergence, with very little additional computational cost, due to the sparse diagonal nature of the preconditioner. The problem gives rise to a square matrix of dimension, $N = 13,340$. The memory used by the direct solver is 90 MB as compared to using the QMR solver with preconditioner, wherein only 4 MB of memory is required.

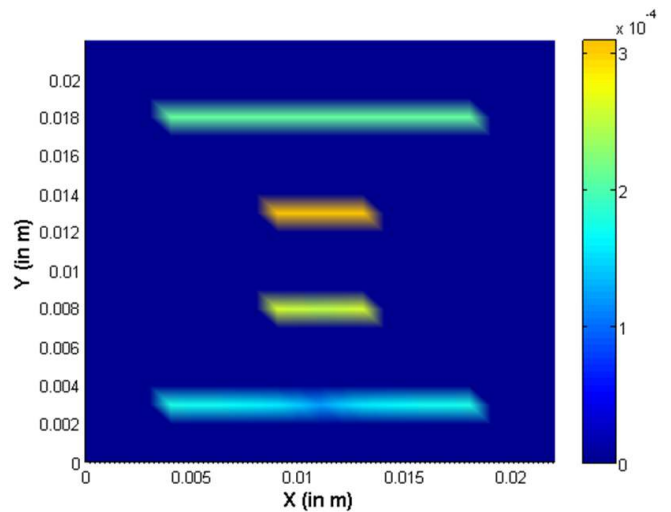


Fig.10 Top-view of x-field component of electric field plotted along the plane 10 μ m above the top metal.

In conclusion, a three-dimensional solver for analyzing metal plane structures in modern packages has been presented and validated. The use of diagonal preconditioner has been demonstrated effecting an improvement in the convergence of the QMR algorithm.

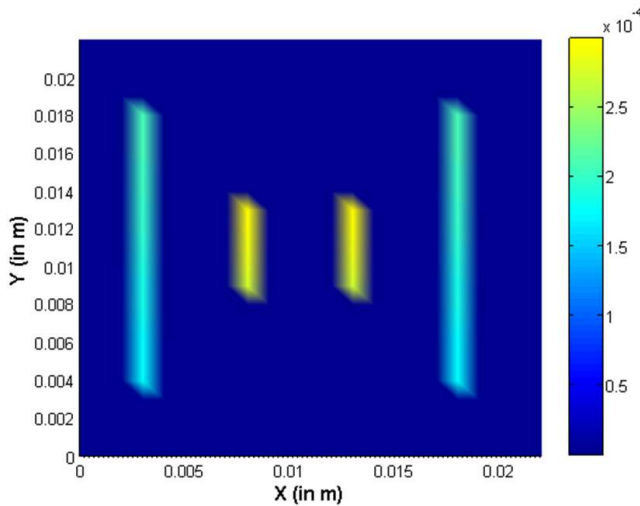


Fig.11 Top-view of y-field component of electric field plotted along the plane $10\mu\text{m}$ above the top metal.

The acceptable increase in memory requirement in the case of the QMR solver as compared to a drastic increase in the memory requirement of direct solver in moving from the first test case to the second implies that large complex structures can be analyzed without being prone to exponential increases in memory. Thus, a fast iterative memory-efficient procedure for obtaining the solution in frequency domain has been demonstrated with superior convergence.

ACKNOWLEDGMENT

This work was supported by the Mixed Signal Design Consortium, Microsystems Packaging Research Center, School of Electrical and Computer Engineering, Georgia Institute of Technology, Atlanta.

REFERENCES

- [1] Frank Y. Yuan, "Electromagnetic modeling and signal integrity simulation of power/ground networks in high speed digital packages and printed circuit boards," *Proc. of 35th Annual ACM IEEE Design Automation Conference*, pp. 421-426, 1998
- [2] Madhavan Swaminathan, E. Engin, *Power integrity modeling and Design for semiconductors and systems*, 1st ed., Prentice Hall PTR, 2007
- [3] Bracken, J.E., Polstyanko S., Raman S., Cendes Z.J., "Efficient full-wave simulation of high-speed printed circuit boards and electronic packages," In *Proc. of IEEE Antennas and Propagation Society International Symposium*, Vol. 3, Iss. 20-25, pp. 3301 – 3304, June 2004
- [4] K. Bharath, E. Engin, M. Swaminathan, K. Uriu, and T. Yamada, "Efficient modeling of package power delivery networks with fringing fields and gap coupling in mixed signal systems. In *Proc. of 15th IEEE EPEP*, pages 59–62, Oct. 2006.
- [5] K. Srinivasan, E. Engin, M. Swaminathan, "Fast FDTD Simulation Using Laguerre Polynomials in MNA Framework," *Proc of IEEE International Symposium on Electromagnetic Compatibility*, pp. 1-6, 9-13 July 2007.
- [6] R. W. Becker, B. McCredie, G. Wilkins, A. Iqbal, "Power Distribution Modeling Power Distribution Modeling of High Performance First Level Computer Packages," *Proc. of IEEE 2nd Topical Meeting on Electrical Performance of Electronic Packaging*, pp. 203-205, 1993.
- [7] Tatsuoh Itoh, Bijan Houshmand, *Time-Domain Methods for Microwave Structures*, IEEE Press, 1998
- [8] Ole Osterby, Zahari Zlatev, *Direct methods for sparse matrices*, New York : Springer-Verlag, 1983.
- [9] Richard S. Varga, *Matrix iterative analysis*, 2nd ed., New York : Springer Verlag, 2000.
- [10] William H. Press, Saul A. Teukolsky, William T. Vetterling, and Brian P. Flannery, *Numerical Recipes in C: the art of scientific computing*, 2nd ed., Cambridge University Press, Cambridge, U.K., 1992
- [11] Freund, Roland W. and Noël M. Nachtigal, "QMR: A quasi-minimal residual method for non-Hermitian linear systems", *SIAM Journal: Numer. Math.*, vol. 60, pp. 315-339, 1991.
- [12] Saad, Youcef and Martin H. Schultz, "GMRES: A generalized minimal residual algorithm for solving nonsymmetric linear systems", *SIAM J. Sci. Stat. Comput.*, vol. 7, no. 3, pp. 856-869, July 1986.
- [13] Y. Saad, *Iterative methods for sparse linear systems*, Philadelphia: SIAM, 2003.
- [14] Al Sharkawy, M., Demir, V., Elsherbeni, A., "An efficient ILU preconditioning for highly sparse matrices constructed using the FDFD method", *IEEE Antennas and Propagation Magazine*, Vol. 49, Iss. 6, pp. 135 – 139, Dec. 2007.